

Predictive coupled-cluster isomer orderings for some Si_nC_m ($m, n \leq 12$) clusters; A pragmatic comparison between DFT and complete basis limit coupled-cluster benchmarks.

Jason N. Byrd,^{1,2, a)} Jesse J. Lutz,^{1, b)} Yifan Jin,¹ Duminda S. Ranasinghe,¹ John A. Montgomery, Jr.,³ Ajith Perera,¹ Xiaofeng F. Duan,^{4,5} Larry W. Burggraf,⁵ Beverly A. Sanders,^{6,1} and Rodney J. Bartlett^{1, c)}

¹⁾ *Quantum Theory Project, University of Florida, Gainesville, Florida 32611, USA*

²⁾ *ENSCO, Inc., 4849 North Wickham Road, Melbourne, Florida 32940, USA*

³⁾ *Department of Physics, University of Connecticut, Storrs, Connecticut 06269, USA*

⁴⁾ *Air Force Research Laboratory DoD Supercomputing Resource Center, Wright-Patterson Air Force Base, OH 45433, USA*

⁵⁾ *Air Force Institute of Technology, Wright-Patterson Air Force Base, Ohio 45433, USA*

⁶⁾ *Department of Computer and Information Science and Engineering, University of Florida, Gainesville, Florida 32611, USA*

The accurate determination of the preferred $\text{Si}_{12}\text{C}_{12}$ isomer is important to guide experimental efforts directed towards synthesizing SiC nano-wires and related polymer structures which are anticipated to be highly efficient exciton materials for opto-electronic devices. In order to definitively identify preferred isomeric structures for silicon carbon nano-clusters, highly accurate geometries, energies and harmonic zero point energies have been computed using coupled-cluster theory with systematic extrapolation to the complete basis limit for set of silicon carbon clusters ranging in size from SiC_3 to $\text{Si}_{12}\text{C}_{12}$. It is found that post-MBPT(2) correlation energy plays a significant role in obtaining converged relative isomer energies, suggesting that predictions using low rung density functional methods will not have adequate accuracy. Utilizing the best composite coupled-cluster energy that is still computationally feasible, entailing a 3-4 SCF and CCSD extrapolation with triple- ζ (T) correlation, the *closo* $\text{Si}_{12}\text{C}_{12}$ isomer is identified to be the preferred isomer in support of previous calculations [J. Chem. Phys. 2015, 142, 034303]. Additionally we have investigated more pragmatic approaches to obtaining accurate silicon carbide isomer energies, including the use of frozen natural orbital coupled-cluster theory and several rungs of standard and double-hybrid density functional theory. Frozen natural orbitals as a way to compute post MBPT(2) correlation energy is found to be an excellent balance between efficiency and accuracy.

I. INTRODUCTION

Recent advancements in the nanoscale design, precision measurement, and coherent control of silicon-based materials are driving rapid developments in electronics,¹ photonics², spintronics,^{3,4} and excitonics.^{5,6} Among the most promising materials, in terms of manufacturing cost, physical durability, and engineering flexibility, is silicon carbide (SiC). SiC has a wide band gap, high thermal conductivity, high breakdown electric field, high saturated electron drift velocity, and it is radiation resistant. This makes it an excellent refractory material for devices which must endure extreme conditions, such as those present in nuclear reactors or interstellar space. Hence, if it can be created efficiently silicon carbide materials are

likely to supplant the bulk silicon crystals currently used in manufacturing microelectronic, photovoltaic, and microelectromechanical system technologies. Furthermore, the diversity of properties exhibited by its many accessible polytypes and nanostructures provides a generous design flexibility which may enable development of novel materials suitable for mainstream production of excitonics, spintronics, and photonics devices.^{4,7}

Large-scale SiC materials design is still at an early stage from the standpoint of both the experimentalist and the theoretician. Preparation of one-dimensional SiC binary core/shell nanowires has for some time been reported,⁸⁻¹⁵ but only very recently was a procedure developed for obtaining highly-crystalline 2-D SiC sheets with nanometer thickness.¹⁶ The latter achievement was inspired by earlier theoretical predictions of the stability of single-layer SiC,¹⁷⁻¹⁹ and this exemplifies the synergy between theory and experiment that has been a common thread in many modern nanoscale materials science advancements. Such breakthroughs stimulate further development of efficient methodologies for the bottom-up theoretical design and engineering of novel nanoscale SiC materials. At the other end of the size spectrum, SiC containing nano-clusters and small molecules are prevalent

^{a)}Electronic mail: byrd.jason@ensco.com

^{b)}Electronic mail: jesse.lutz.ctr@afit.edu; This research was supported in part by an appointment to the Faculty Research Participation Program at U.S. Air Force Institute of Technology (AFIT), administered by the Oak Ridge Institute for Science and Education through an interagency agreement between the U.S. Department of Energy and AFIT.

^{c)}Electronic mail: rodbartl@ufl.edu

in the interstellar medium. Because of the difficulties in experimental replication of the interstellar environment, there is a great demand for theory to provide any comparable molecular data.

Nearly all stable Si_nC_m molecules do not resemble their bulk SiC counterpart. Solid-state SiC consists of mostly extended chains of alternating Si and C atoms, while Si_nC_m clusters tend to be segregated into carbon- and silicon-rich regions, with sporadic linkage through Si-C bonds. When n is small, silicon link to the periphery as single atoms or clusters, and when n is large, the silicon network spans the carbon moiety. The relative stability of Si_mC_n molecules tends to maximize with $n = m$, and, in particular, the $\text{Si}_{12}\text{C}_{12}$ molecule has become motivating due to its ability to form different polymer chains as well as 2D and 3D networks by Si-Si bonding.²⁰ However, predicting in advance the most energetically-favorable arrangement of the atoms in such systems can be very challenging.

Ab initio methods are an excellent tool for sampling the configuration space of a molecular cluster to find the global minimum. As the most accurate methods are extremely computationally taxing, identification of more efficient approaches is desired and this can be done by comparison with benchmark values, if possible. Unfortunately the structural details of large Si_nC_m clusters are not yet documented, but parameters for smaller clusters have for some time been known from interstellar and laboratory spectroscopy. These measurements form the basis for a systematic study which may help determine the most efficient methods for studying larger clusters or perhaps even periodic SiC systems.

The first observation of visible-range interstellar absorption bands corresponding to Si_nC_m clusters were reported in 1926 by Merrill²¹ and Sanford,²² and these bands were later correctly attributed to the SiC_2 molecule by Kleman.²³ Other small silicon carbide clusters have been observed using radio astronomy including SiC ,²⁴ rhomboidal SiC_3 ,²⁵ and linear SiC_4 .²⁶ Gas-phase IR spectra measured in the laboratory helped further characterize ground-state Si_nC_m geometries, providing definitive structural parameters for SiC ,²⁷ triangular SiC_2 ,²⁸⁻³⁰ triangular SiC_2 ,³¹ linear SiC_4 ,^{32,33} SiC_n ($n > 4$),³⁴⁻³⁶ triangular Si_2C ,^{37,38} rhombic Si_2C_2 ,³⁹ linear SiC_3Si ,⁴⁰⁻⁴² linear SiC_4Si ,⁴³ Si_2C_5 ,⁴⁴ rhomboidal Si_3C ,⁴⁵ pentagonal Si_3C_2 ,⁴⁶ and silicon-rich Si_nC (with $n = 3-8$)⁴⁷ and Si_nC_m (with $n + m = 6$) clusters.⁴⁸ Computational modeling has also been performed by several groups in order to describe small ground-state Si_nC_m clusters,⁴⁹⁻⁶⁷ heterofullerenes,⁶⁸⁻⁷¹ cage structures,⁷² silafullerenes,⁷³ and graphene-silicene bilayers.^{74,75}

In 2010, several low-lying isomers of the Si_nC_m ($m, n \leq 4$) clusters were studied to determine the most energetically stable ground-state structures.⁷⁶ At that time the reported structures reinforced all known spectroscopic interpretations, but since then Truong et al. measured a ground-state geometry for Si_4C in disagreement with

the predictions.⁴⁷ This discrepancy also called into question the reliability of other calculations performed on medium-sized Si_nC_m clusters ($m, n \leq 12$).⁷⁷ Since those results led to the intriguing prediction of the existence of a stable, cage-like *closo*- $\text{Si}_{12}\text{C}_{12}$ structure,⁷⁸ it is of great interest to know whether the reported DFT isomer energy-ordering is correct and *closo*- $\text{Si}_{12}\text{C}_{12}$ is in fact the most thermodynamically stable isomer.

This work has two related motivations. Firstly, before embarking on an effort to synthesize the *closo*- $\text{Si}_{12}\text{C}_{12}$ molecule and its polymeric extensions,²⁰ one needs to definitively confirm that it is, in fact, the most stable isomer. If this initial prediction is proven to be in question, more difficult and less efficient kinetic synthesis approaches will become necessary. Secondly, once highly-accurate coupled-cluster results are obtained, the effectiveness of more pragmatic approaches for the treatment of large Si_nC_m clusters can be explored. In this way it is desirable to identify a DFT-based method which can offer a much more efficient yet reliable alternative for determining the lowest-energy isomer searches and other computational predictive studies on Si_nC_m clusters and their polymeric analogue.

II. ELECTRONIC STRUCTURE CALCULATIONS

We performed all reported electronic structure calculations using the serial ACESII,⁷⁹ and parallel ACESIII,⁸⁰ Aces4,⁸¹ GAMESS,^{82,83} ORCA,⁸⁴ and NWCHEM⁸⁵ *ab initio* quantum chemistry packages. Correlation calculations were performed using the ACES family of *ab initio* programs on the NAVY DSRC Cray XC30 Shepard and ARL DSRC Cray XC40 Excalibur. Density functional theory (DFT) calculations were performed on the University of Florida HiPerGator cluster and NAVY DSRC Cray XC30 Shepard using GAMESS and NWCHEM, while double-hybrid density functional theory calculations were performed using ORCA on a local work station. Correlation and DFT calculations performed here use Dunning’s correlation consistent family of basis sets (cc-pVnZ and tight function variant cc-pV(n+d)Z, $n=D,T,Q,5$) optionally with diffuse functions (aug-) and with weighted core-valence functions (cc-pwCVnZ).⁸⁶⁻⁸⁸ All double-hybrid (DH) DFT calculations used the resolution-of-the-identity (RI) approximation in the DFT⁸⁹ and MBPT(2) calculation using the def2-QZVP⁹⁰ basis. Correlation calculations in this work assume the frozen-core approximation where all carbon 1s and silicon 1s2s2p orbitals are frozen at the SCF level and dropped from the correlation space unless explicitly stated otherwise. Throughout this work, a very tight grid is employed, the JANS=2 grid in GAMESS and xfine in NWCHEM. Geometry optimizations and single point energy calculations were performed using a large variety of methods including second-order many-body perturbation theory with the Møller-Plesset partitioning (MBPT(2)),

linear coupled-cluster doubles (LCCD),^{91–94} coupled-cluster theory with singles and doubles (CCSD),⁹⁵ and CCSD with perturbative triples^{96–98} (CCSD(T)), and some DFT functionals. Throughout MAX refers to the maximum unsigned error, MUEs as the mean unsigned error, and RMS as the root mean square of the error.

When computing the relative isomer energies for large molecular systems using conventional *ab initio* methods, it is convenient to take advantage of energy additivity to analyze the calculated energies by orders of perturbation theory. This enables the systematic inclusion of higher-order estimates of the correlation energy, often illustrated by the *ab initio* hierarchy, MBPT(2)<LCCD<CCSD<CCSD(T)<...<FCI. As a function of basis set the analogous hierarchy is $D\zeta < T\zeta < Q\zeta < \dots < \infty\zeta$, where the latter term is the infinite basis set idealization. To obtain the best possible isomer energies for our available computational resources, the individual energy contributions computed with a given basis set can be separated and added to form an aggregate total energy. Summarizing our notation, the MBPT(2) correlation energy is represented by

$$\Delta\text{MBPT}(2) = E(\text{MBPT}(2)) - E(\text{SCF}) \quad (1)$$

with higher order contributions similarly defined as

$$\Delta\text{CCSD} = E(\text{CCSD}) - E(\text{SCF}), \quad (2)$$

$$\Delta(\text{T}) = E(\text{CCSD}(\text{T})) - E(\text{CCSD}), \quad (3)$$

and

$$\Delta\text{CC} = E(\text{CCSD}(\text{T})) - E(\text{MBPT}(2)) \quad (4)$$

as the post MBPT(2) correlation energy.

As an alternative to including the correlation energy from a small basis or using a large amount of computational resources to obtain large basis results, it is possible to approximate the largest basis set correlation energies at the cost of a small basis using the frozen natural orbital (FNO) method.^{99,100} The FNO scheme is a way to truncate the virtual orbital space in a post-MBPT(2) (CCSD and beyond) calculation with a p^4 (p is the amount of virtual space truncated) computational savings. As is evident by the polynomial dependence on the number of virtual orbitals, truncating even small portions of the virtual space can lead to tremendous computational savings. Our goal of calculating accurate isomerization energies is an ideal target for the FNO method¹⁰¹ due to the favorable cancellation of error to be obtained from the energy differences of structurally similar isomers.

The FNO method works by ordering the virtual orbitals based on the MBPT(2) virtual-virtual density occupation numbers then truncating the remaining space based on an occupation number threshold criteria; details of this ordering and truncation can be found in the FNO references.^{99,100,102} In our experience^{99–101} virtual space truncation using a 1×10^{-4} threshold (which usually means a removal of 30–35% of the virtual orbitals)

is a good balance between accuracy and efficiency.¹⁰³ The general energy decomposition notation for FNO energies is

$$\Delta_{\text{FNO}}(\text{T}) = E_{\text{FNO}}(\text{CCSD}(\text{T})) - E_{\text{FNO}}(\text{CCSD}), \quad (5)$$

and

$$\Delta_{\text{FNOCC}} = E_{\text{FNO}}(\text{CCSD}(\text{T})) - E(\text{MBPT}(2)). \quad (6)$$

As a note, the $\Delta_{\text{FNO}}(\text{T})$ energy is computed using the truncated virtual FNO T amplitudes, which incurs only a small error.^{101,102}

It is well known that the basis set convergence of post-MBPT(2) correlation is much faster than the SCF and second-order contribution.¹⁰⁴ Because each contribution to the total energy has a different basis set dependence, we can estimate the effects of taking the total energy to the complete basis set limit (CBS) by examining the basis set dependence of each contribution ($E(\text{SCF})$, $\Delta\text{MBPT}(2)$, ΔCCSD , and $\Delta(\text{T})$) individually. Extrapolation of smaller basis set energies is a very effective way to estimate the CBS limit without requiring the use of very large basis sets to directly obtain an energy near the CBS limit. We employ the linear extrapolation formula of Schwenke¹⁰⁵

$$E_{\infty}^n(\text{SCF}) = E_{n-1}(\text{SCF}) + F_{n-1,n}^{\text{SCF}}(E_n(\text{SCF}) - E_{n-1}(\text{SCF})) \quad (7)$$

$$\Delta_{\infty}^n\text{M} = \Delta_{n-1}\text{M} + F_{n-1,n}^{\text{M}}(\Delta_n\text{M} - \Delta_{n-1}\text{M}) \quad (8)$$

and the cubic extrapolation formula of Helgaker *et al.*¹⁰⁶

$$\Delta_{\infty}^n\text{MBPT}(2) = \frac{n^3\Delta_n\text{MBPT}(2) - (n-1)^3\Delta_{n-1}\text{MBPT}(2)}{n^3 - (n-1)^3} \quad (9)$$

to obtain CBS estimates of the SCF, MBPT(2) and higher order (ΔCCSD , and $\Delta(\text{T})$) contributions to the total energy. Here $E_n(\text{M})$, $\Delta_n\text{MBPT}(2)$ and $\Delta_n(\text{M})$ refer to that energy contribution computed with the cc-pVnZ basis while $F_{n-1,n}^{\text{M}}$ is a tabulated quantity.¹⁰⁵ There are a number of ways to assemble the CBS estimates of the SCF and correlation energies which vary in accuracy and computational cost. Based on what is currently computationally feasible, we define a best estimate of the CBS extrapolated energy to be

$$E_{\text{CBS}}(\text{Best}) = E_{\infty}^5(\text{SCF}) + \Delta_{\infty}^4(\text{CCSD}) + \Delta_3(\text{T}) + \text{ZPE} \quad (10)$$

where ZPE is the harmonic zero point energy (ZPE) computed at the MBPT(2)/cc-pVTZ level of theory. For smaller clusters we additionally investigate the ΔCCSD core-valence correlation energy (ΔCV using the corresponding cc-pwCVnZ basis set) and compute an MBPT(2)-level fine-structure relativistic correction (ΔFS). Other, more approximate estimates for the CBS total energy employed in this work are

$$\text{MBPT}(2) :: \Delta_2\text{CC} = E_\infty^4(\text{SCF}) + \Delta_\infty^4(\text{MBPT}) + \Delta_2\text{CC} + \text{ZPE}, \quad (11)$$

$$\text{MBPT}(2) :: \Delta_{\text{FNO}}\text{CC} = E_\infty^4(\text{SCF}) + \Delta_\infty^4(\text{MBPT}) + \Delta_{\text{FNO}}\text{CC} + \text{ZPE}, \quad (12)$$

$$\text{CCSD} :: \Delta_n(\text{T}) = E_\infty^4(\text{SCF}) + \Delta_\infty^4(\text{CCSD}) + \Delta_n(\text{T}) + \text{ZPE}, \quad (13)$$

$$\text{CCSD} :: \Delta_{\text{FNO}}(\text{T}) = E_\infty^4(\text{SCF}) + \Delta_\infty^4(\text{CCSD}) + \Delta_{\text{FNO}}(\text{T}) + \text{ZPE}. \quad (14)$$

Each of which uses a cc-pV{T,Q}Z extrapolation to estimate the SCF and leading order correlation energy CBS limit, with higher order correlation contributions included at either the cc-pVDZ, FNO/cc-pVTZ or full cc-pVTZ level.

A computationally attractive method for computing the energies of large molecules is DFT, which has had a long history of competition with wave-function theory. An extensive examination of the performance of density functional theory in the calculation of structures and energies of Si_nC_m clusters is beyond the scope of this work. However we have included a survey of relative isomer energies computed by a number of common functionals including B3LYP^{107,108} (using VWN5), cam-QTP(0,0),¹⁰⁹ cam-QTP(0,1),¹¹⁰ $\omega\text{B97X-D2}$,^{111,112} M06-2X,¹¹³ and M11¹¹⁴ in our results to provide a point of comparison for future efforts. We also provide values computed using the B2-PLYP,^{115,116} B2GP-PLYP,¹¹⁷ DSD-BLYP,¹¹⁸ DSD-PBEP86,¹¹⁹ and PWPB95¹²⁰ DH-DFT. The -D2 (2006) and -D3 (2010) Grimme dispersion corrections^{121,122} were employed as denoted above.

III. COMPUTATIONAL RESULTS AND DISCUSSION

In this study we develop and apply accurate yet efficient computational protocols for the determination of structural parameters and energetic rankings of low-lying Si_nC_m isomers. To this end, we set forth several objectives: (1) establish a list of approaches which efficiently determine structural parameters for small Si_nC_m clusters, (2) verify the level of accuracy achieved by the benchmark composite method (Eq. 10) when used to compute isomer energy differences for small Si_nC_m clusters, (3) identify those computational approaches that provide a qualitatively correct energy-ordering of optimized structures of small and medium Si_nC_m isomers by comparing with benchmark-quality results, and (4) recommend pragmatic procedures for the determination of qualitatively correct isomer energy ordering which scales from small through medium Si_nC_m clusters, up to and including the target $\text{Si}_{12}\text{C}_{12}$ system.

A. Efficiently Optimizing Geometries of Si_nC_m Clusters with $n, m \leq 2$

Initially we investigated the accuracy of various combinations of method and basis set for describing the ground-state structural parameters of the four smallest

($n, m \leq 2$) Si_nC_m clusters. The results of geometry optimizations performed on the ^3X surface of SiC and on the ^1X surfaces of SiC_2 , Si_2C , and Si_2C_2 are compared in Table I where the MUEs of the collective optimized bond lengths and collective optimized bond angles are reported for ground-state SiC, SiC_2 , Si_2C , and Si_2C_2 clusters. Benchmark bond distances and bond angles were taken to be those resulting from optimization at the highest level of theory considered, CCSD(T)/aug-cc-pV(Q+d)Z. The full set of MUEs determined for each system at the various levels of theory can be found in the supplemental material.¹²³

When basis sets of D ζ -quality are employed, every wave-function method considered produced large MUEs of over 3.0 pm and 7.0 degrees for the bond lengths and angles, respectively. At this basis set level the DFT functionals outperform the wave-function methods we tested by at least a factor of two, producing MUEs of 0.7–1.5 pm and 0.3–1.1 degrees. The computational efficiency of DFT makes small-basis B3LYP, M11, and $\omega\text{B97X-D}$ good candidates for obtaining structural parameters when large-basis wave-function approaches are unaffordable. It is yet to be seen whether these methods also produce accurate isomer energy orderings.

Improving the basis sets to T ζ quality caused uniform improvement in the performance of all relevant wave-function methods, with associated MUEs decreasing to within 1.0 pm and 0.7 degrees for bond lengths and angles, respectively. In contrast, the MUEs of the DFT methods did not uniformly improve when increasing the basis set size. This introduces uncertainty regarding the expected performance of DFT methods for larger systems, since the number of basis functions necessarily grows relative to the system size. However, this small basis accuracy illustrates that for such DFT methods the basis set is readily saturated. Of the more reliable wave-function methods tested, MBPT(2) is the most computationally tractable, identifying it as a leading candidate for use in optimizations.

In general, increasing the basis set size beyond the standard cc-pVTZ produced diminishing returns. The inclusion of diffuse or tight- d functions is shown in Table I to be non-essential at both the D ζ or T ζ level for all methods tested, resulting in improvements in MUEs of, at best, 0.1–0.3 pm or 0.1–0.3 degrees for the bond lengths and angles, respectively. Similarly, improving

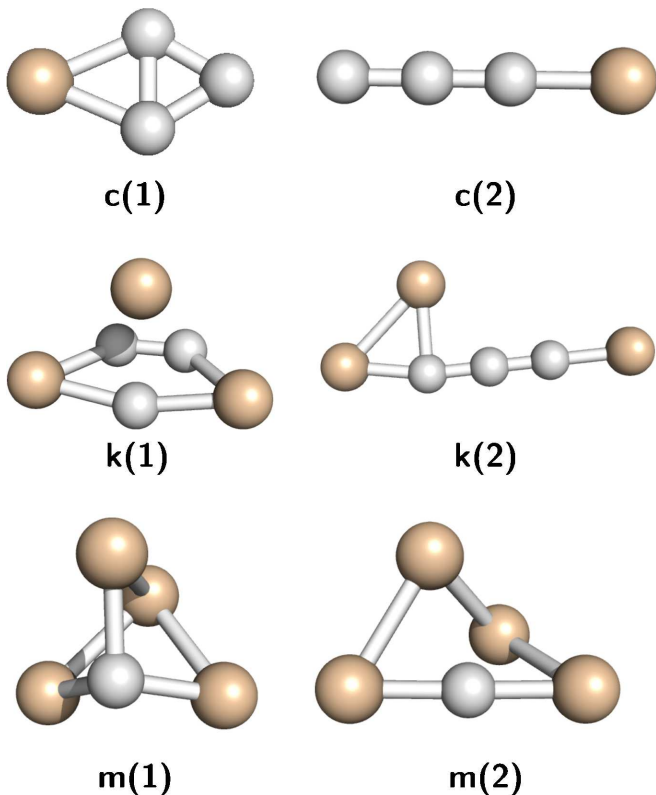


FIG. 1. The lowest-lying isomers of SiC_3 , Si_3C_3 , and Si_4C , as optimized using MBPT(2)/VTZ.

the basis set from $\text{T}\zeta$ - to the more expensive $\text{Q}\zeta$ -quality generally did not produce a worthwhile reduction in the MUEs. In light of these findings, the optimization approaches employed in the remainder of this work are limited to having either cc-pVDZ or cc-pVTZ basis sets. The MBPT(2)/ cc-pVTZ optimized geometries for all Si_mC_n clusters with $m \leq n \leq 4$ can be found in the supplemental material.¹²³

B. Validating a Composite Method for Generating Benchmark Values

Small Si_nC_m clusters were also used to validate the accuracy of the composite method outlined in Eq. 10, which is a useful tool for benchmarking the performance of other approaches. Our strategy for this task is to examine individual contributions to the total isomer energy differences and study their convergence behavior as a function of basis set size. The SiC_3 , Si_3C_3 , and Si_4C systems are considered in this way, since these three systems have been previously identified in the literature as having contentious lowest-energy isomer configurations.^{76,124} In conformance with the notation of Duan *et al.*,⁷⁶ the two lowest-lying isomeric structures are labeled as c1 and c2 for SiC_3 , k1 and k2 for Si_3C_3 , and m1 and m2 for Si_4C . The corresponding geometries were optimized at

the MBPT(2)/ cc-pVTZ level and are sketched in Figure 1 for reference.

Leading contributions to the isomer energy differences, as obtained for the SiC_3 , Si_3C_3 , and Si_4C isomer pairs, are presented in Table II. Focusing first on SiC_3 , only small changes are found when moving from the cc-pVDZ to the cc-pVTZ basis sets for most of the individual energies, with the exception of the SCF and ΔCCSD quantities. By then stepping back to examine the ΔCCSD convergence behavior for all three molecular systems, it is clear that $\text{Q}\zeta$ -quality calculations are generally required before values are converged to within 1 kcal/mol of the CBS limit. Due to the small extra computational effort involved, $\{\text{TZ}, \text{QZ}\}$ correlation energy extrapolations were routinely performed, as were large-basis SCF calculations.

Considering now the magnitude of the various energy differences computed at the cc-pVDZ level, several appear relatively small. For this set of systems, the ΔCV and ΔFS contributions never contribute more than 0.5 kcal/mol to their respective energy differences. Since the relative size of both of these corrections is expected to decrease in moving to larger SiC clusters, it is probably safe to omit them. Finally, the ZPE values are reasonably converged at the MBPT(2)/ cc-pVDZ level, but can also be conveniently be obtained at the MBPT(2)/ cc-pVTZ level following a geometry optimization at the same level. On the basis of these observations for small clusters, it appears that the composite method given by Eq. 10 will provide isomer enthalpy differences approaching ~ 1 kcal/mol for larger SiC clusters.

C. Accurately ordering the relative isomer energy for Si_nC_m clusters with $n, m \leq 2$

Another important consideration when developing an approach for searching for the lowest-energy isomer is whether the level of theory used for geometry optimizations will also provide an appropriate energy-ordering of the optimized structures. Often when only the structure of the global minimum is of interest, all other stationary points are discarded once the leading candidate is identified. This can be problematic however, since the energy-ordering resulting from the optimization method can be misleading, even in the case where very accurate structural parameters are returned. To test this we focus on the challenging case of the two lowest-lying structures of Si_4C , which are known to interchange depending on the level of theory employed.

In Table III several values are compiled which compare the quality of the geometry optimization and relative energies provided by various levels of theory. A set of eight bond lengths (four from each Si_4C structure) and a set of ten angles and dihedrals (five from each Si_4C structure) are used to produce MUEs corresponding to the equilibrium bond lengths and angles. As before, these MUEs are compiled by comparing against parameters de-

terminated at the highest level of theory employed, which in this case was CCSD(T)/cc-pVTZ. These quantities show similar trends to those reported in Table I. While some DFT methods in conjunction with the cc-pVDZ basis can provide efficient approaches for obtaining relatively good geometrical parameters, only the LCCD/cc-pVTZ method is accurate enough to produce MUEs of bond lengths and angles within 1.0 pm and 1.0 angles of the CCSD(T)/VTZ benchmark.

Also reported in Table III are the relative energies of each isomer pair, as computed in two ways. The first ($\Delta E(\text{opt})$) employed the same level of theory as is used for the optimization and the second ($\Delta E(\text{Best})$) applied the composite approach given by Eq. 10 to the same optimized structures. The $\omega\text{B97X-D}$, B3LYP, and LCCD methods alone failed to unambiguously separate the energies of the two isomers. The M11 and MBPT(2) approaches predicted correct qualitative isomer energy orderings, but excluding CCSD(T)/cc-pVDZ none of the optimization approaches successfully predicted the energy difference to within 1 kcal/mol of the target CCSD(T)/cc-pVTZ value.

Summarizing our findings for the small Si_nC_m clusters, reliable geometries are generally obtained using wave-function methods together with the cc-pVTZ basis set. When such methods become computationally intractable, slightly less robust structures can be obtained in a more efficient manner using DFT methods with the cc-pVDZ basis set. While none of the optimization methods tested here reliably predicted CCSD(T) isomer energy orderings to within chemical accuracy, the M11 and MBPT(2) approaches were found to at least provide an unambiguous and correct energy ordering of the Si_4C isomers. Of these two methods only the MBPT(2) structures result in energy differences within 10% of benchmark values when the high-accuracy composite method is subsequently applied. Thus, while MBPT(2) may not provide raw Si_nC_m energies matching the accuracy of CC theory, the MBPT(2) method is able to provide both (1) reliable structures for performing subsequent high-accuracy calculations and (2) raw energies which give an unambiguous and qualitatively correct isomer energy orderings. This led us to choose MBPT(2)/cc-pVTZ as our default method for performing geometry optimizations on the larger clusters in the following sections.

D. Accurate Isomers Energy orderings for Si_nC_n clusters with $n = 4, 5, 6$

In addition to benchmarking smaller silicon carbide systems, we are able to employ high level coupled-cluster methods on the medium sized Si_nC_n clusters. Previous calculations⁷⁷ have performed a systematic search of the configuration space for $n = 4, \dots, 12$ and identified four lowest structures for each cluster size to be close in energy using B3LYP. In order to validate and benchmark the relative isomer energies the $n = 4, 5$ and 6 clusters are

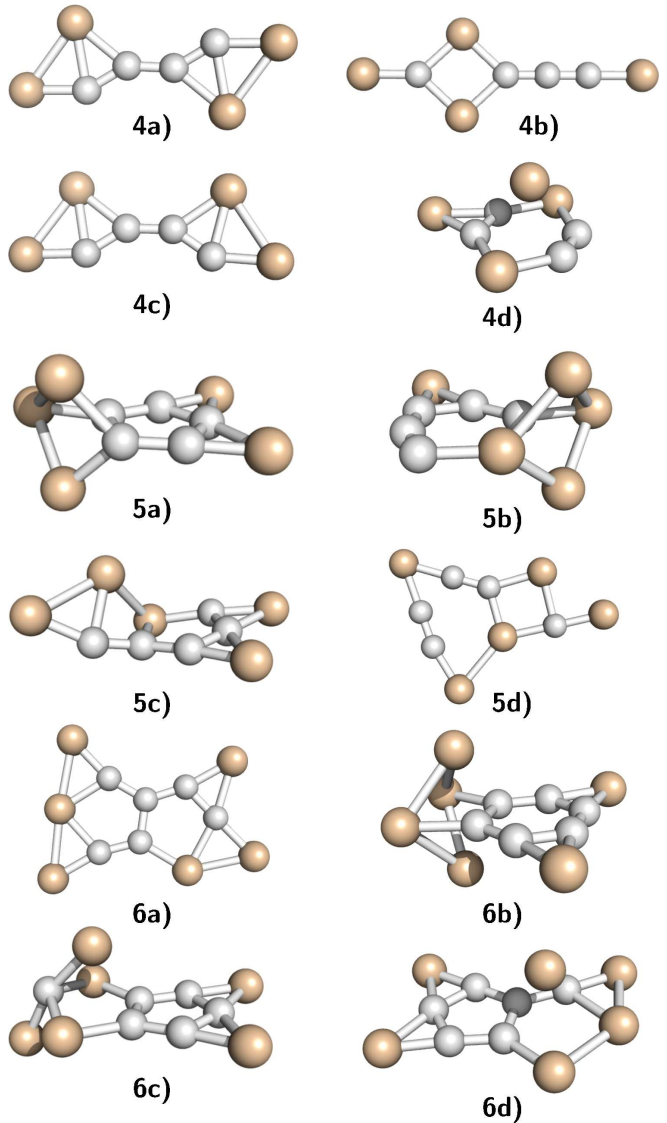


FIG. 2. Schematic structures for the four lowest Si_nC_n ($n = 4, \dots, 6$) clusters, MBPT(2)/cc-pVTZ optimized coordinates are provided in the supplemental material.¹²³

selected for re-examination. Optimized geometries and Hessians are computed with MBPT(2) (for the coupled-cluster and DH-DFT calculations) or DFT (each single point is evaluated at the geometry predicted by that DFT functional) using the cc-pVTZ basis set. Schematic diagrams of the twelve silicon carbide clusters can be found in Fig. 2. The MBPT(2)/cc-pVTZ optimized geometries for all twelve Si_nC_n clusters can be found in the supplemental material.¹²³

The $E_{\text{CBS}}(\text{Best})$, MBPT(2):: $\Delta_2\text{CC}$, and CCSD:: $\Delta_n(\text{T})$ relative isomer energies of the Si_nC_n ($n = 4, 5, 6$) clusters are reported in Table IV using the MBPT(2) geometries. From a pragmatic perspective, the $E_{\text{CBS}}(\text{Best})$ (Eq. 10) composite energy does not differ significantly from the CCSD:: $\Delta_n(\text{T})$ results that require a computationally expensive cc-pV5Z SCF

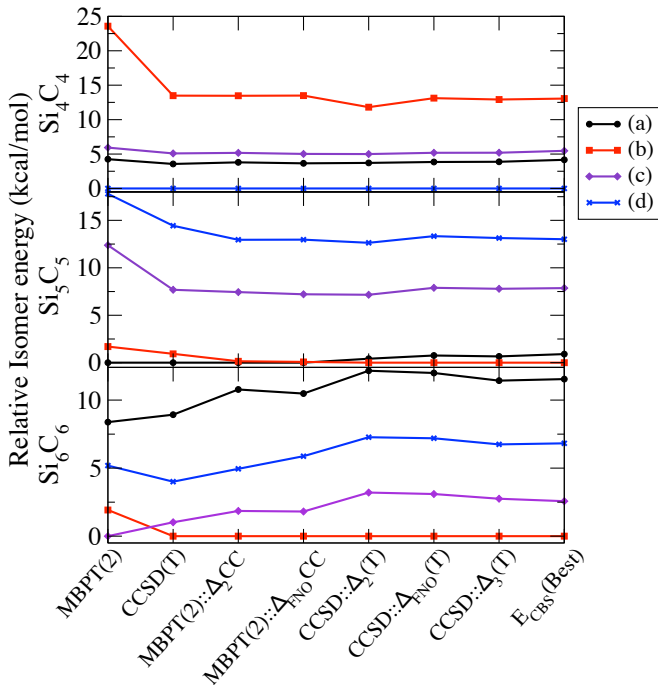


FIG. 3. Relative isomer energies for the four lowest Si_nC_n ($n = 4, 5, 6$) clusters.

calculation. In Fig. 3 the relative isomer energies are plotted to demonstrate their convergence as the quality of the composite model is increased. From Fig. 3 it is readily apparent that calculating the $\Delta(T)$ contribution using the cc-pVDZ basis or FNO with the cc-pVTZ basis is nearly sufficient to obtain quantitative results. Using only the MBPT(2) CBS energies with small bases and FNO ΔCC corrections is not sufficient to completely reproduce the Si_5C_5 predicted isomer ordering despite having excellent agreement for the other clusters. As the difference between 5(a) and 5(b) is ~ 0.75 kcal/mol this discrepancy is not unexpected as it would be overly generous to assign that level of accuracy to an approximate CBS model applied to a system of this size.

The DH-DFT relative isomer energies compared to the $E_{\text{CBS}}(\text{Best})$ reference value are given in Table V. The DH-DFT single point energies are obtained at the MBPT(2)/cc-pVTZ geometry and include the corresponding MBPT(2)/cc-pVTZ ZPE correction. Overall the DH-DFT results track the reference values very well, and are a significant improvement over canonical MBPT(2)/cc-pVQZ (see Table V). The DSD-PBEP86 flavor performed notably well across the 12 reference values.

Presented in Table VI are the DFT relative isomer energies as computed with lower rung functionals. The results with the various functionals are mixed, with B3LYP incorrectly predicting the relative energies for any of the mid sized clusters with an RMS (MAX) error of 7 (12.5) kcal/mol while the recently developed¹¹⁰ cam-QTP(0,1) and $\omega\text{B97X-D}$ functionals correctly predict the energy

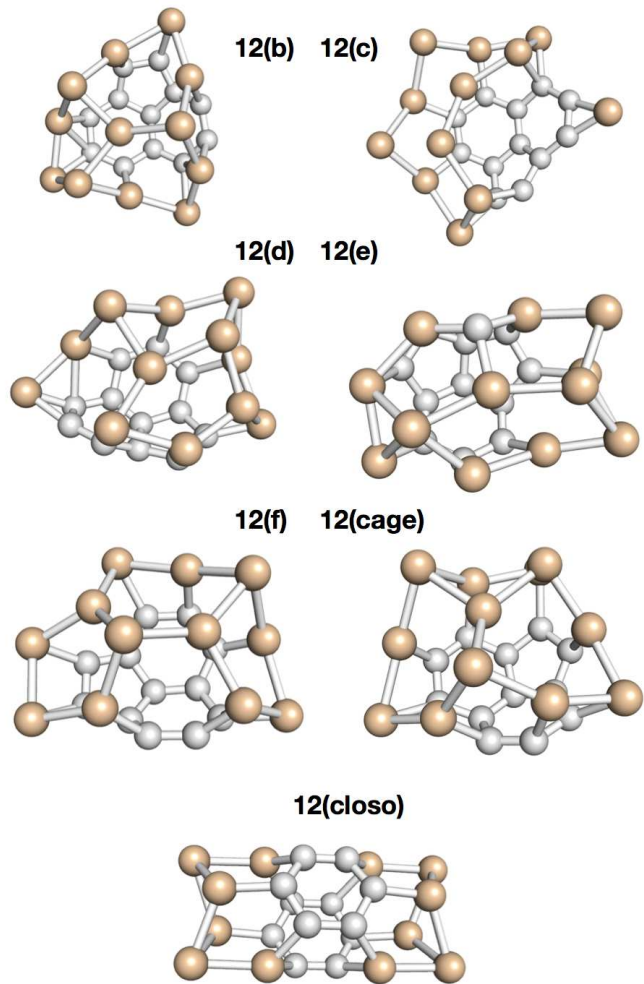


FIG. 4. Schematic structures for the seven lowest $\text{Si}_{12}\text{C}_{12}$ clusters, MBPT(2)/cc-pVTZ optimized coordinates are provided in the supplemental material.¹²³

orders in some cases with more acceptable RMS (MAX) errors of 2.8 (7.2) and 2.3 (4.5) kcal/mol respectively. Specifically the Si_5C_5 cluster is a difficult case for all the DFT functionals where the 5(a)-5(b) gap is somewhat greater than the coupled-cluster result and in the wrong order where 5(a) is predicted to be preferred. From an accuracy/efficiency argument the DH-DFT methods provide qualitatively accurate orderings with reasonably quantitative accuracy when compared with our best CBS coupled-cluster results.

E. Isomer Energies of $\text{Si}_{12}\text{C}_{12}$

The reliability of various levels of theory for obtaining the optimized geometries of smaller silicon carbon clusters are assessed in the previous section, providing a highly accurate framework of model CBS energy decom-

position schemes that will now be used to address the question of isomer ordering and thermodynamic stability of the $\text{Si}_{12}\text{C}_{12}$ clusters. We focus our attention on six cage like configurations⁷⁷ and the highly symmetric and compact *closo* structure⁷⁸ previously reported to be the lowest preferred isomers of $\text{Si}_{12}\text{C}_{12}$. Illustrations of these seven structures are given in Fig. 4.

Optimized geometries and Hessians are computed using DFT/cc-pVTZ and MBPT(2)/cc-pVTZ, the latter used in the calculation of the model CBS energy and for the DH-DFT calculations. The MBPT(2)/cc-pVTZ optimized geometries for all seven $\text{Si}_{12}\text{C}_{12}$ clusters can be found in the supplemental material.¹²³ We forgo computing the $E_{\infty}^5(\text{SCF})$ extrapolated energy as it is clear from Table IV that the $E_{\infty}^4(\text{SCF})$ is quite sufficient for the larger clusters. The two most computationally challenging aspects of the calculation that remain are the MBPT(2)/cc-pVTZ Hessian and CCSD/cc-pVQZ single point energy. The Hessian is particularly onerous due to the lack of symmetry in most of the cage structures, resulting in many degrees of freedom. The CCSD/cc-pVQZ single point energy is a large calculation with ~ 1400 basis functions included. Fortunately calculations of this size are becoming routine^{101,125-127} for the parallel ACES programs.

The relative isomer energies are presented in Tables VII, VIII, and IX. As computed by DFT, the relative energy between the *closo* and various cage structures ranges evenly from ~ 4 to ~ 20 kcal/mol with the *closo* predicted to be preferred. The M06-2X and M11 functionals are outliers in this set, with a *closo*-cage difference nearing ~ 12 kcal/mol. A computed difference of ~ 4 kcal/mol for a system this size using DFT is less definitive than otherwise would be desired, but is none the less suggestive just as previous calculations concluded.^{77,78} This trend is amplified when examining the DH-DFT results, where the *closo*-cage isomer energy gap now ~ 10 kcal/mol. It should be noted that these large $\text{Si}_{12}\text{C}_{12}$ DH-DFT calculations were performed on commodity workstations

Turning to the proposed CBS models the difference between the *closo* and other cage structures remains now at ~ 14 kcal/mol, a much stronger indication that the *closo* is the $\text{Si}_{12}\text{C}_{12}$ thermodynamically preferred isomer. It is evident from Table IX that the simple CBS model, MBPT(2):: Δ_{FNOCC} , is entirely sufficient for the selected $\text{Si}_{12}\text{C}_{12}$ structures to decisively predict the large difference between the *closo* and other cages. Furthermore this approach is significantly faster to compute and suggests that more approximate approaches using MBPT(2) as the primary source of correlation could be very successful when applied to larger silicon carbide systems. The claim that MBPT(2) correlation with small corrections from higher-order contributions is sufficient for the larger SiC clusters is supported by the very good agreement of the DH-DFT results as compared to the CCSD:: $\Delta_3(\text{T})$ reference value.

While CCSD/cc-pVQZ energies are obtainable for

the seven structures considered here, such a calculation might not be practical for much larger systems, much less their infinite polymer analogues. Hence it is useful that the Δ_{FNOCC} correction to the MBPT(2) extrapolated energy is quite sufficient to obtaining accurate coupled-cluster relative energies as such a calculation is quick to perform using more readily available hardware (in our case the FNO calculations were performed on the HiPerGator 2.0 system). Should even the FNO be impractical, then qualitative and quantitative energies can nonetheless be obtained from a DH-DFT calculation. The alternative of using the M11 functional is also viable, as it is the only tested DFT functional to get close to the coupled-cluster energy ordering and spacing with the caveat that the M11 functional was unable to correctly predict the smaller (Si_nC_n , $n \leq 6$) silicon-carbon clusters.

IV. CONCLUSIONS

In this work we have predicted the lowest energy isomer for some silicon carbide clusters, Si_nC_m ($m, n \leq 12$), using extensive coupled-cluster calculations including converged estimates to the complete basis set limit. Our computed isomer order and energy differences for the Si_nC_n ($4 \leq n \leq 6$) clusters (see Table IV) differs significantly from previous B3LYP results.⁷⁷ The source of the DFT discrepancy with our best CC based calculations is attributed to the inadequacies of B3LYP as most of the alternative DFT functions examined here are far more accurate (Table VI). In particular the cam-QTP(0,1) density functional, based on a reparametrization of cam-B3LYP, outperforms the canonical functional. Additionally we have included double-hybrid DFT isomerization energies, which can be considered as a reasonable compromise between accuracy, theoretical rigor and efficiency. In addition to computing a best possible CBS coupled-cluster isomerization energy, we also provide a systematic study (see Fig. 3) of the convergence for various approximate composite energy models to clearly illustrate the basis set and perturbation order important to describing small SiC clusters.

The *closo* $\text{Si}_{12}\text{C}_{12}$ structure is confirmed to be the lowest preferred isomer, consistent with previous B3LYP calculations.⁷⁸ However most DFT functionals do not accurately reproduce the CBS coupled-cluster predicted isomer orderings and energy differences for the various cage structures. The best possible CBS coupled-cluster composite model, $E_{\text{CBS}}(\text{Best})$ (Eq. 10), entails a 4-5 ζ SCF, and 3-4 ζ CCSD extrapolation with a 3 ζ (T) single point energy performed at the MBPT(2)/cc-pVTZ computed geometry. The $E_{\text{CBS}}(\text{Best})$ calculations include a CCSD/cc-pVQZ calculation (with ~ 1400 basis functions) which we are able to easily perform even for the largest SiC clusters considered here due to the efficiency of the massively parallel Aces quantum chemistry packages.

More pragmatically however, utilizing standard DFT to compute silicon carbon isomer energies is shown to be highly unreliable, with RMS errors of ~ 10 kcal/mol even for the cam-QTP(0,1) and ω B97X-D functionals which were performed for smaller clusters. In order to obtain accurate isomer predictions it is found that a large basis MBPT(2) calculation with some portion of post MBPT(2) correlation energy is necessary for ~ 1 kcal/mol accuracy. Along this line, the double-hybrid density functional theory DSD-PBEP86-D3 and PWPB95-D3 (using the def2-QZVP basis) methods perform well, as do *ab initio* CBS MBPT(2) results corrected by a FNO coupled-cluster calculation. Both of these more pragmatic composite energies only require modest computational resources for even the largest silicon carbon clusters considered here.

Looking forward to much larger Si_nC_n clusters, alternatives to performing very large basis CCSD calculations is desirable. As large basis MBPT(2) results are becoming increasingly available for very large systems, through the use of parallel implementations or approximations like the resolution-of-the-identity, composite CBS energies or alternatives like DH-DFT are viable when accurate ground state energetics are required. The relative errors for the SiC clusters examined here between the approximate models and our best results are on the order of 1 – 2 kcal/mol, leaving the choice in which calculation to perform is between a balance of theoretical rigor and efficiency. Our conservative recommendation for future isomerization studies of very large Si_nC_m clusters is the MBPT(2) :: Δ_{FNOCC} model (Eq. 12), which favors theoretical rigor as increasing system size can occasionally lead to unanticipated complications with DFT based models. In cases where DH-DFT or wave-function methods are not affordable, it was shown here that M11 more frequently provides an adequate description of the structure and relative energetics of SiC clusters as compared with other commonly-used standard DFT functionals.

V. ACKNOWLEDGEMENTS

This work was supported by funding from the U.S. Department of Defense High Performance Computing Modernization Program and a grant of computer time at the U.S. NAVY and U.S. Army Research Lab DoD Supercomputing Resource Centers. Additionally, JJJ was supported in part by an appointment to the Faculty Research Participation Program at U.S. Air Force Institute of Technology (AFIT), administered by the Oak Ridge Institute for Science and Education through an interagency agreement between the U.S. Department of Energy and AFIT. The views expressed in this work are those of the authors and do not reflect the official policy or position of the United States Air Force, Department of Defense, or the United States Government.

REFERENCES

- ¹F. A. Zwanenburg, A. S. Dzurak, A. Morello, M. Y. Simmons, L. C. L. Hollenberg, G. Klimeck, S. Rogge, S. N. Coppersmith, and M. A. Eriksson, *Rev. Mod. Phys.* **85**, 961 (2013).
- ²J. Leuthold, C. Koos, and W. Freude, *Nat. Photonics* **4**, 535 (2010).
- ³R. Jansen, *Nat. Mater.* **11**, 400 (2012).
- ⁴M. Widmann, S.-Y. Lee, T. Rendler, N. T. Son, H. Fedder, S. Paik, L.-P. Yang, N. Zhao, S. Yang, I. Booker, A. Denisenko, M. Jamali, S. A. Momenzadeh, I. Gerhardt, T. Ohshima, A. Gali, E. Janzén, and J. Wrachtrup, *Nat. Mater.* **14**, 164 (2015).
- ⁵G. D. Scholes and G. Rumbles, *Nat. Mater.* **5**, 683 (2006).
- ⁶S. W. Koch, M. Kira, G. Khitrova, and H. M. Gibbs, *Nat. Mater.* **5**, 523 (2006).
- ⁷M. Radulaski, T. M. Babinec, S. Buckley, A. Rundquist, J. Provine, K. Alassaad, G. Ferro, and J. Vučković, *Opt. Express* **21**, 32623 (2013).
- ⁸X. T. Zhou, R. Q. Zhang, H. Y. Peng, N. G. Shang, N. Wang, I. Bello, C. S. Lee, and S. T. Lee, *Chem. Phys. Lett.* **332**, 215 (2000).
- ⁹Y. Ryu, B. Park, Y. Song, and K. J. Yong, *J. Cryst. Growth* **271**, 99 (2004).
- ¹⁰W. Yang, H. Araki, C. C. Tang, S. Thaveethavorn, A. Kohyama, H. Suzuki, and T. Noda, *Adv. Mater.* **17**, 1519 (2005).
- ¹¹J. P. Alper, M. Vincent, C. Carraro, and R. Maboudian, *Appl. Phys. Lett.* **100**, 163901 (2012).
- ¹²M. Ollivier, L. Latu-Romain, M. Martin, S. David, A. Mantoux, E. Bano, V. Soulière, G. Ferro, and T. Baron, *J. Cryst. Growth* **363**, 158 (2013).
- ¹³N. F. F. B. Nazarudin, N. J. B. M. Noor, S. A. Rahman, and B. T. Goh, *J. Lumin.* **157**, 149 (2015).
- ¹⁴B. T. Goh and S. A. Rahman, *Mater. Chem. Phys.* **147**, 974 (2014).
- ¹⁵R. Rurali, *Phys. Rev. B* **71**, 205405 (2005).
- ¹⁶Y. X. S. Chabi, H. Chang and Y. Zhu, *Nanotechnology* **27**, 075602 (2016).
- ¹⁷P. Mélinon, B. Masenelli, F. Tournus, and A. Perez, *Nat. Mater.* **6**, 479 (2007).
- ¹⁸E. Bekaroglu, M. Topsakal, S. Cahangirov, and S. Ciraci, *Phys. Rev. B* **81**, 075433 (2010).
- ¹⁹P. Li, R. Zhou, and X. C. Zeng, *Nanoscale* **6**, 11685 (2014).
- ²⁰X. F. Duan and L. W. Burggraf, *J. Chem. Phys.* **144**, 114309 (2016).
- ²¹P. W. Merrill, *Publ. Astron. Soc. Pac.* **38**, 175 (1926).
- ²²R. F. Sanford, *Publ. Astron. Soc. Pac.* **38**, 177 (1926).
- ²³B. Klemm, *Astrophys. J.* **123**, 162 (1956).
- ²⁴J. Cernicharo, C. A. Gottlieb, M. Guelin, P. Thaddeus, and J. M. Vrtilik, *Astrophys. J.* **341**, L25 (1989).
- ²⁵A. J. Apponi, M. C. McCarthy, C. A. Gottlieb, and P. Thaddeus, *Astrophys. J.* **516**, L103 (1999).
- ²⁶M. Ohishi, N. Kaifu, and K. K. et al., *Astrophys. J.* **345**, L83 (1989).

- ²⁷P. F. Bernath, S. A. Rogers, L. C. O'Brien, C. R. Brazier, and A. D. McLean, *Phys. Rev. Lett.* **60**, 197 (1988).
- ²⁸R. A. Shepherd and W. R. M. Graham, *J. Chem. Phys.* **82**, 4788 (1985).
- ²⁹D. L. Michalopoulos, M. E. Geusic, P. R. R. Langridge-Smith, and R. E. Smalley, *J. Chem. Phys.* **80**, 3556 (1984).
- ³⁰J. D. Presilla-Márquez and W. R. M. Graham, *J. Chem. Phys.* **95**, 5612 (1991).
- ³¹J. D. Presilla-Márquez, W. R. M. Graham, and R. A. Shepherd, *J. Chem. Phys.* **93**, 5224 (1990).
- ³²P. A. Withey and W. R. Graham, *J. Chem. Phys.* **96**, 4068 (1992).
- ³³A. V. Orden, R. A. Provencal, T. F. Giesen, and R. J. Saykally, *Chem. Phys. Lett.* **237**, 77 (1995).
- ³⁴X. D. Ding, S. L. Wang, C. M. L. Rittby, and W. R. M. Graham, *J. Chem. Phys.* **110**, 11214 (1999).
- ³⁵X. D. Ding, S. L. Wang, C. M. Rittby, and W. R. M. Graham, *J. Phys. Chem. A* **104**, 3712 (2000).
- ³⁶T. G. Lê, C. M. Rittby, and W. R. M. Graham, *J. Chem. Phys.* **140**, 064314 (2014).
- ³⁷Z. H. Kafafi, R. H. Hauge, L. Fredin, and J. L. Margrave, *J. Phys. Chem.* **87**, 797 (1983).
- ³⁸N. J. Reilly, P. B. Changala, J. H. Baraban, D. L. Kokkin, J. F. Stanton, and M. C. McCarthy, *J. Chem. Phys.* **142**, 231101 (2015).
- ³⁹J. D. Presilla-Márquez, S. C. Gay, C. M. L. Rittby, and W. R. M. Graham, *J. Chem. Phys.* **102**, 6354 (1995).
- ⁴⁰J. D. Presilla-Márquez and W. R. M. Graham, *J. Chem. Phys.* **100**, 181 (1994).
- ⁴¹A. V. Orden, T. F. Giesen, R. A. Provencal, and R. J. Saykally, *J. Chem. Phys.* **101**, 10237 (1994).
- ⁴²S. Thorwirth, J. Krieg, V. Lutter, I. Keppeler, S. Schlemmer, M. E. Harding, J. Vázquez, and T. F. Giesen, *J. Mol. Spectrosc.* **270**, 75 (2011).
- ⁴³J. D. Presilla-Márquez, C. M. Rittby, and W. R. M. Graham, .
- ⁴⁴T. G. Lê, C. M. Rittby, and W. R. M. Graham, *J. Chem. Phys.* **141**, 044315 (2014).
- ⁴⁵J. D. Presilla-Márquez and W. R. M. Graham, *J. Chem. Phys.* **96**, 6509 (1992).
- ⁴⁶J. D. Presilla-Márquez and W. R. M. Graham, *J. Chem. Phys.* **104**, 2818 (1996).
- ⁴⁷N. X. Truong, M. Savoca, D. J. Harding, A. Fielicke, and O. Dopfer, *Phys. Chem. Chem. Phys.* **17**, 18961 (2015).
- ⁴⁸M. Savoca, A. Lagutschenkow, J. Langer, D. J. Harding, A. Fielicke, and O. Dopfer, *J. Phys. Chem. A* **117**, 1158 (2013).
- ⁴⁹C. M. L. Rittby, *J. Chem. Phys.* **96**, 6768 (1992).
- ⁵⁰C. M. L. Rittby, *J. Chem. Phys.* **100**, 175 (1994).
- ⁵¹R. S. Grev and H. F. Schaefer, *J. Chem. Phys.* **80**, 3552 (1984).
- ⁵²R. S. Grev and H. F. Schaefer, *J. Chem. Phys.* **82**, 4126 (1985).
- ⁵³R. S. Grev and H. F. Schaefer, *Chem. Phys. Lett.* **119**, 111 (1985).
- ⁵⁴R. S. G. I. L. Alberts and H. F. Schaefer, *J. Chem. Phys.* **93**, 5046 (1990).
- ⁵⁵Z. Y. Jiang, X. H. Xu, H. S. Wu, F. Q. Zhang, and Z. H. Jin, *J. Mol. Struct.* **589**, 103 (2002).
- ⁵⁶Z. Y. Jiang, X. H. Xu, H. S. Wu, F. Q. Zhang, and Z. H. Jin, *Chin. J. Struct. Chem.* **22**, 459 (2003).
- ⁵⁷H. S. W. Z. Y. Jiang, X. H. Xu and Z. H. Jin, *J. Phys. Chem. A* **107**, 10126 (2003).
- ⁵⁸Z. Y. Jiang, X. H. Xu, H. S. Wu, F. Q. Zhang, and Z. H. Jin, *J. Mol. Struct.* **624**, 61 (2003).
- ⁵⁹Z. Y. Jiang, X. H. Xu, H. S. Wu, F. Q. Zhang, and Z. H. Jin, *J. Mol. Struct.* **621**, 279 (2003).
- ⁶⁰J. Hou and B. Song, *J. Chem. Phys.* **128**, 154304 (2008).
- ⁶¹B. Song, Y. Yong, J. Hou, and P. He, *Eur. Phys. J. D* **59**, 399 (2010).
- ⁶²J. Zhang, W. C. Lu, Q. J. Zang, L. Z. Zhao, C. Z. Wang, and K. M. Ho, *J. Phys.: Condens. Matter* **23**, 205305 (2011).
- ⁶³S. Erkoç and L. Turker, *Physica E* **8**, 50 (2000).
- ⁶⁴Q. X. Li, W. C. Lu, Q. J. Zang, L. Z. Zhao, C. Z. Wang, and K. M. Ho, *Comput. Theor. Chem.* **963**, 439 (2011).
- ⁶⁵S. Hunsicker and R. O. Jones, *J. Chem. Phys.* **105**, 5048 (1996).
- ⁶⁶A. D. Zdetsis, G. Froudakis, M. Muhlhauser, and H. Thummel, *J. Chem. Phys.* **104**, 2566 (1996).
- ⁶⁷M. Azeezulla Nazrulla, K. Joshi, S. Israel, and S. Krishnamurthy, *Physica E* **76**, 173 (2016).
- ⁶⁸M. R. Momeni and F. A. Shakib, *Chem. Phys. Lett.* **492**, 137 (2010).
- ⁶⁹M. N. Huda and A. K. Ray, *Chem. Phys. Lett.* **457**, 124 (2008).
- ⁷⁰R. Scipioni, M. Matsubara, E. Ruiz, C. Massobrio, and M. Boero, *Chem. Phys. Lett.* **510**, 14 (2011).
- ⁷¹M. Yu, C. S. Jayanthi, and S. Y. Wu, *Nanotechnology* **23**, 235705 (2012).
- ⁷²P. Pochet, L. Genovese, D. Caliste, I. Rousseau, S. Goedecker, and T. Deutsch, *Phys. Rev. B* **82**, 035431 (2010).
- ⁷³J. Tillmann, J. H. Wender, U. Bahr, M. Bolte, H.-W. Lerner, M. C. Holthausen, and M. Wagner, *Angew. Chem. Int. Ed.* **54**, 5429 (2015).
- ⁷⁴M. Neek-Amal, A. Sadeghi, G. R. Berdiyrov, and F. M. Peeters, *Appl. Phys. Lett.* **103**, 261904 (2013).
- ⁷⁵F. M. P. G.R. Berdiyrov, M. Neek-Amal and A. van Duin, *Phys. Rev. B* **89**, 024107 (2014).
- ⁷⁶X. Duan, J. Wei, L. Burggraf, and D. Weeks, *Comput. Mater. Sci.* **47**, 630 (2010).
- ⁷⁷X. F. Duan, L. W. Burggraf, and L. Huang, *Molecules* **18**, 8591 (2013).
- ⁷⁸X. F. Duan and L. W. Burggraf, *J. Chem. Phys.* **142**, 034303 (2015).
- ⁷⁹J. F. Stanton, J. Gauss, S. A. Perera, A. Yau, J. D. Watts, M. Nooijen, N. Oliphant, P. G. Szalay, W. J. Lauderdale, S. R. Gwaltney, S. Beck, A. Balková,

- D. E. Bernholdt, K.-K. Baek, P. Rozyczko, H. Sekino, C. Huber, J. Pittner, and R. J. Bartlett, "ACESII is a product of the quantum theory project, university of florida," Integral packages included are VMOL (Almöf, J and Taylor, P. R.) VPROPS (Taylor, P. R.) and ABACUS (Helgaker, T. and Jensen, H. J. Aa. and Jørgensen P. and Olsen J. and Taylor P. R.).
- ⁸⁰V. Lotrich, N. Flocke, M. Ponton, A. Yau, A. Perera, E. Deumens, and R. Bartlett, *J. Chem. Phys.* **128**, 2722 (2008).
- ⁸¹B. A. Sanders, N. Jindal, J. N. Byrd, V. F. Lotrich, D. Lyakh, N. Flocke, A. Perera, and R. J. Bartlett, "Aces4 pre-alpha release," <https://github.com/UFPParLab>.
- ⁸²M. W. Schmidt and K. K. Baldridge and J. A. Boatz and S. T. Elbert and M. S. Gordon and J. J. Jensen and S. Koseki and N. Matsunaga and K. A. Nguyen and S. Su and T. L. Windus and M. Dupuis and J. A. Montgomery, Jr., *J. Comput. Chem.* **14**, 1347 (1993).
- ⁸³M. S. Gordon and M. W. Schmidt, in *Theory and Applications of Computational Chemistry, the First Forty Years*, edited by C. E. Dykstra, G. Frenking, K. S. Kim, and G. E. Scuseria (Elsevier, Amsterdam, 2005) pp. 1167–1189.
- ⁸⁴F. Neese, *Wiley Interdisciplinary Reviews: Computational Molecular Science* **2**, 73 (2011).
- ⁸⁵M. Valiev, E. J. Bylaska, N. Govind, K. Kowalski, T. P. Straatsma, H. J. J. Van Dam, D. Wang, J. Nieplocha, E. Aprà, T. L. Windus, and W. A. de Jong, *Comp. Phys. Comm.* **181**, 1477 (2010).
- ⁸⁶T. Dunning Jr, *J. Chem. Phys.* **90**, 1007 (1989).
- ⁸⁷D. Woon and T. Dunning Jr, *J. Chem. Phys.* **98**, 1358 (1993).
- ⁸⁸T. Dunning, Jr., K. Peterson, and A. Wilson, *J. Chem. Phys.* **114**, 9244 (2001).
- ⁸⁹F. Weigend, M. Kattannek, and R. Ahlrichs, *J. Chem. Phys.* **130**, 164106 (2009).
- ⁹⁰F. Weigend, F. Furche, and R. Ahlrichs, *J. Chem. Phys.* **119**, 12753 (2003).
- ⁹¹R. J. Bartlett, *Annu. Rev. Phys. Chem.* **32**, 359 (1981).
- ⁹²A. G. Taube and R. J. Bartlett, *J. Chem. Phys.* **130**, 144112 (2009).
- ⁹³R. J. Bartlett, M. Musial, V. F. Lotrich, and T. Kus, in *Recent Progress in Coupled-Cluster Methods*, Vol. 11, edited by P. Carsky, J. Paldus, and J. Pittner (Springer, Dordrecht, 2010) Chap. 1, pp. 1–34.
- ⁹⁴J. N. Byrd, V. Rishi, A. Perera, and R. J. Bartlett, *J. Chem. Phys.* **143**, 164103 (2015).
- ⁹⁵G. D. Purvis III and R. J. Bartlett, *J. Chem. Phys.* **76**, 1910 (1982).
- ⁹⁶M. Urban, J. Noga, S. J. Cole, and R. J. Bartlett, *J. Chem. Phys.* **83**, 4041 (1985).
- ⁹⁷K. Raghavachari, G. W. Trucks, J. A. Pople, and M. Head-Gordon, *Chem. Phys. Lett.* **157**, 479 (1989).
- ⁹⁸J. D. Watts, J. Gauss, and R. J. Bartlett, *J. Chem. Phys.* **98**, 8718 (1993).
- ⁹⁹A. G. Taube and R. J. Bartlett, *Coll. Czech. Chem. Comm.* **70**, 837 (2005).
- ¹⁰⁰A. G. Taube and R. J. Bartlett, *J. Chem. Phys.* **128**, 164101 (2008).
- ¹⁰¹J. N. Byrd, N. Jindal, R. W. Molt, Jr., R. J. Bartlett, B. A. Sanders, and V. F. Lotrich, *Mol. Phys.* **113**, 1 (2015).
- ¹⁰²A. E. DePrince III and C. D. Sherrill, *J. Chem. Theory Comput.* **9**, 293 (2012).
- ¹⁰³Care must be made to not select a threshold that would incorrectly remove degenerate virtual orbitals.
- ¹⁰⁴J. A. Platts, J. G. Hill, K. E. Riley, J. Řezáč, and P. Hobza, *J. Chem. Theory Comput.* **9**, 330 (2013).
- ¹⁰⁵D. Schwenke, *J. Chem. Phys.* **122**, 014107 (2005).
- ¹⁰⁶T. Helgaker, W. Klopper, H. Koch, and J. Noga, *J. Chem. Phys.* **106**, 9639 (1997).
- ¹⁰⁷A. Becke, *J. Chem. Phys.* **98**, 5648 (1993).
- ¹⁰⁸P. Stephens, F. Devlin, C. Chabalowski, and M. Frisch, *J. Phys. Chem.* **98**, 11623 (1994).
- ¹⁰⁹P. Verma and R. J. Bartlett, *J. Chem. Phys.* **140**, 18A534 (2014).
- ¹¹⁰Y. Jin and R. J. Bartlett, in press.
- ¹¹¹J.-D. Chai and M. Head-Gordon, *J. Chem. Phys.* **128**, 084106 (2004).
- ¹¹²J.-D. Chai and M. Head-Gordon, *Phys. Chem. Chem. Phys.* **10**, 6615 (2008).
- ¹¹³Y. Zhao, N. E. Schultz, and D. G. Truhlar, *Journal of Chemical Theory and Computation* **2**, 364 (2006).
- ¹¹⁴R. Peverati and D. G. Truhlar, *J. Phys. Chem. Lett.* **2**, 2810 (2011).
- ¹¹⁵S. Grimme, *J. Chem. Phys.* **124**, 034108 (2006).
- ¹¹⁶T. Schwabe and S. Grimme, *Acc. Chem. Res.* **41**, 569 (2008).
- ¹¹⁷A. Karton, A. Tarnopolsky, J.-F. Lameère, G. Schatz, and J. M. L. Martin, *J. Phys. Chem. A* **112**, 12868 (2008).
- ¹¹⁸S. Kozuch, D. Gruzman, and J. M. L. Martin, *J. Phys. Chem. C* **114**, 20801 (2010).
- ¹¹⁹S. Kozuch and J. M. L. Martin, *Phys. Chem. Chem. Phys.* **13**, 20104 (2011).
- ¹²⁰L. Goerigk and S. Grimme, *J. Chem. Theory Comput.* **7**, 291 (2011).
- ¹²¹S. Grimme, *J. Comput. Chem.* **27**, 1787 (2006).
- ¹²²S. Grimme, J. Antony, S. Ehrlich, and H. Krieg, *J. Chem. Phys.* **132**, 154104 (2010).
- ¹²³See supplementary material at [URL will be inserted by AIP] for.
- ¹²⁴M. Steglich and J. P. Maier, *Astrophys J.* **801**, 119 (2015).
- ¹²⁵R. W. Molt, Jr., T. Watson, Jr., A. P. Bazanté, and R. Bartlett, *J. Phys. Chem. A* **117**, 3467 (2013).
- ¹²⁶J. N. Byrd, R. J. Bartlett, and J. A. Montgomery Jr., *J. Phys. Chem. A* **118**, 1706 (2014).
- ¹²⁷Y. Jin, A. Perera, V. F. Lotrich, and R. J. Bartlett, *Chem. Phys. Lett.* **629**, 76 (2015).

TABLE I. Mean unsigned errors (MUEs) of bond lengths and bond angles for the ground states of SiC, SiC₂, Si₂C, and Si₂C₂, as optimized at various levels of theory. All values are MUEs reported with respect to the CCSD(T)/aug-cc-pV(Q+d)Z results.

Method	Basis set ^a						
	VDZ	AVDZ	AV(D+d)Z	VTZ	AVTZ	AV(T+d)Z	AV(Q+d)Z
MUE of optimized bond lengths in pm							
ω B97X-D	0.8	1.0	1.1	1.5	1.6	1.7	1.9
B3LYP	1.3	1.1	1.0	1.0	1.0	1.1	1.1
M11	0.7	1.5	1.1	1.9	1.8	1.7	1.2
MBPT(2)	3.9	4.2	3.7	0.8	0.9	0.6	0.3
LCCD	3.4	3.6	3.1	0.7	0.7	0.7	1.1
CCSD	3.5	3.7	3.2	0.5	0.4	0.4	1.0
CCSD(T)	4.4	4.5	4.1	0.7	0.9	0.6	0.0
MUE of optimized bond angles in degrees							
ω B97X-D	1.1	0.8	0.9	1.0	1.0	1.0	0.4
B3LYP	0.8	0.7	0.8	0.9	0.9	0.9	0.8
M11	0.6	0.8	0.3	0.8	1.0	1.0	0.9
MBPT(2)	7.4	8.4	7.2	0.7	0.5	0.5	0.7
LCCD	7.8	9.9	9.1	0.4	0.2	0.3	0.5
CCSD	8.5	10.2	9.4	0.4	0.5	0.4	0.3
CCSD(T)	11.0	12.7	12.0	0.2	0.5	0.2	0.0

^a The basis sets cc-pVnZ, aug-cc-pVnZ, and aug-cc-pV(n+d)Z are abbreviated as VnZ, AVnZ, and AV(n+d)Z, respectively.

TABLE II. Basis-set convergence of various leading contributions to the relative energies of the two lowest-lying structural isomers of SiC₃, Si₃C₃, and Si₄C. For the meaning of the quantities see the text. Energies are in kcal/mol.

Energy contribution	Basis set			
	cc-pVDZ	cc-pVTZ	cc-pVQZ	CBS ^a
SiC ₃ isomer energy difference, E(c2)-E(c1)				
$E(\text{SCF})$	-10.2	-11.4	-11.1	-11.0
ΔCCSD	14.3	17.2	18.0	18.5
$\Delta(\text{T})$	1.2	1.2	1.3	1.4
ZPE	-1.1	-1.3		
ΔCV	-0.1	-0.4		
ΔFS	-0.00	-0.01		
$E_{\text{CBS}}(\text{Best})$				7.6 ^b
Si ₃ C ₃ isomer energy difference, E(k2)-E(k1)				
$E(\text{SCF})$	-10.2	-7.2	-6.9	-6.5
ΔCCSD	11.9	14.8	15.7	16.3
$\Delta(\text{T})$	1.3	1.4		
ZPE	-0.7	-0.8		
ΔCV	0.5			
ΔFS	-0.08			
$E_{\text{CBS}}(\text{Best})$				10.4 ^b
Si ₄ C isomer energy difference, E(m2)-E(m1)				
$E(\text{SCF})$	-7.7	-7.4	-7.4	-7.3
ΔCCSD	7.4	7.8	8.1	8.3
$\Delta(\text{T})$	2.6	2.6		
ZPE	-0.3	-0.4		
ΔCV	0.1			
ΔFS	0.01			
$E_{\text{CBS}}(\text{Best})$				3.2 ^b

^a Computed as $E_{\infty}^5(\text{SCF})$ and $\Delta_{\infty}^4\text{CC}$ from Eqs. 7 and 8, respectively.

^b See Eq. 10.

TABLE III. Measures of the accuracy of various levels of theory for the geometry optimization of Si₄C isomers. Structural parameters, including bond lengths (in pm) and bond angles and dihedrals (in degrees), are reported as MUEs with respect to benchmark values optimized at the CCSD(T)/cc-pVTZ level. Isomer energy differences are reported in kcal/mol.

Method	Basis set	MUE(R_e) ^a	MUE(θ_e) ^b	$\Delta E(\text{opt})$ ^c	$E_{\text{CBS}}(\text{Best})$ ^d
ω B97X-D	cc-pVDZ	7.0	2.4	-0.07	7.95
	cc-pVTZ	2.3	2.7	0.01	2.39
B3LYP	cc-pVDZ	2.4	1.0	-0.02	3.85
	cc-pVTZ	1.1	0.9	-0.00	3.62
M11	cc-pVDZ	0.9	1.5	1.83	4.52
	cc-pVTZ	2.1	1.2	1.71	4.07
MBPT(2)	cc-pVDZ	2.1	1.0	4.78	3.29
	cc-pVTZ	1.4	1.2	5.79	3.18
LCCD	cc-pVDZ	2.9	0.5	-0.56	3.45
	cc-pVTZ	0.8	0.6	0.31	3.27
CCSD(T)	cc-pVDZ	3.6	0.4	2.64	3.73
	cc-pVTZ	0.0	0.0	3.55	3.52

^a The mean unsigned error of equilibrium bond lengths of the optimized m1 and m2 isomers.

^b The mean unsigned error of equilibrium bond angles of the optimized m1 and m2 isomers.

^c The isomer energy difference $[E(m2)-E(m1)]$, computed using the specified optimization method.

^d Isomer energy difference $[E(m2)-E(m1)]$, computed using Eq. 10.

TABLE IV. Relative energies (in kcal/mol) for the four lowest Si_nC_n ($n = 4, 5, 6$) clusters using the MBPT(2)/cc-pVTZ reference geometry. See text for details of the extrapolation methods used.

Si _n C _n	CCSD(T) ^a	MBPT(2)::		CCSD::		CCSD::		$E_{\text{CBS}}(\text{Best})$
		$\Delta_2\text{CC}$	$\Delta_{\text{FNO}}\text{CC}$	$\Delta_2(\text{T})$	$\Delta_{\text{FNO}}(\text{T})$	$\Delta_3(\text{T})$		
4(a)	3.56	3.80	3.66	3.71	3.85	3.87	4.16	
4(b)	13.49	13.47	13.49	11.81	13.12	12.92	13.06	
4(c)	5.09	5.17	5.02	5.00	5.18	5.19	5.46	
4(d)	0.00	0.00	0.00	0.00	0.00	0.00	0.00	
5(a)	0.00	0.00	0.00	0.41	0.76	0.66	0.90	
5(b)	0.93	0.15	0.08	0.00	0.00	0.00	0.00	
5(c)	7.68	7.44	7.21	7.16	7.89	7.79	7.87	
5(d)	14.43	12.95	12.97	12.64	13.33	13.14	13.01	
6(a)	8.93	10.78	10.48	12.16	11.99	11.43	11.54	
6(b)	0.00	0.00	0.00	0.00	0.00	0.00	0.00	
6(c)	1.02	1.85	1.81	3.21	3.10	2.75	2.57	
6(d)	4.00	4.95	5.88	7.27	7.20	6.75	6.82	
MAX	2.82	1.88	1.06	1.25	0.53	0.29		
RMS	1.24	0.66	0.57	0.52	0.26	0.15		

^a Single point computed with the cc-pVTZ basis

Si_nC_n	B2PLYP	B2GP-PLYP	DSD-BLYP	DSD-PBEP86	PWPB95	MBPT(2) ^a	$E_{\text{CBS}}(\text{Best})^b$
	-D3	-D3	-D3	-D3	-D3		
4(a)	0.00	1.05	1.51	2.17	3.69	4.25	4.16
4(b)	3.90	7.08	10.07	12.82	14.05	23.57	13.06
4(c)	1.66	2.24	2.80	3.66	5.82	5.94	5.46
4(d)	1.76	0.00	0.00	0.00	0.00	0.00	0.00
5(a)	2.28	3.02	2.80	1.04	0.00	0.00	0.90
5(b)	0.00	0.00	0.00	0.00	0.21	1.70	0.00
5(c)	6.92	9.08	10.24	10.44	11.06	12.38	7.87
5(d)	8.73	11.90	13.04	15.56	18.75	17.80	13.01
6(a)	2.58	5.70	6.14	9.38	13.41	8.38	11.54
6(b)	0.38	0.00	0.00	0.00	0.00	1.92	0.00
6(c)	0.00	0.39	1.03	2.75	4.17	0.00	2.57
6(d)	3.45	4.40	5.14	6.02	6.65	5.19	6.82
MAX	9.16	5.98	5.40	2.57	5.74	10.52	
RMS	4.46	3.00	2.36	1.47	2.07	3.88	

^a Single point computed with the cc-pVQZ basis.

^b See Eq. 10.

TABLE V. Relative energies (in kcal/mol) for the four lowest Si_nC_n ($n = 4, 5, 6$) clusters using density-fitted resolution-of-the-identity double-hybrid DFT as compared to $E_{\text{CBS}}(\text{Best})$ at the MBPT(2)/cc-pVTZ reference geometry.

Si_nC_n	B3LYP	cam-QTP(0,0)	cam-QTP(0,1)	$\omega\text{B97X-D}$	M06-2X	M11	$E_{\text{CBS}}(\text{Best})^a$
4(a)	0.00	3.21	3.07	0.61	5.10	6.33	4.16
4(b)	0.56	6.13	9.63	10.52	16.91	23.98	13.06
4(c)	2.00	4.63	4.36	1.94	6.84	7.79	5.46
4(d)	10.14	0.00	0.00	0.00	0.00	0.00	0.00
5(a)	0.00	0.00	0.00	0.00	0.00	0.00	0.90
5(b)	1.16	6.06	7.15	4.51	5.07	4.80	0.00
5(c)	2.58	5.39	6.83	7.50	11.93	11.17	7.87
5(d)	1.96	13.27	15.69	15.86	23.36	25.62	13.01
6(a)	0.00	16.50	15.17	11.94	18.40	20.00	11.54
6(b)	2.30	0.00	0.00	0.00	0.00	0.00	0.00
6(c)	1.30	5.06	4.09	3.45	5.86	6.30	2.57
6(d)	3.18	10.34	9.09	6.93	8.74	9.95	6.82
MAX	12.49	6.93	7.15	4.51	10.35	12.61	
RMS	7.04	3.37	2.81	2.27	4.37	5.90	

^a See Eq. 10.

TABLE VI. Relative energies (in kcal/mol) for the four lowest Si_nC_n ($n = 4, 5, 6$) clusters using DFT as compared to $E_{\text{CBS}}(\text{Best})$ at the MBPT(2)/cc-pVTZ reference geometry.

Si_nC_n	B3LYP	cam-QTP(0,0)	cam-QTP(0,1)	$\omega\text{B97X-D}$	M06-2X	M11	CCSD:: $\Delta_3(\text{T})^b$
12(b)	6.52	3.00	6.47	6.59	28.54	17.85	19.21
12(c)	7.06	2.36	5.12	6.99	19.48	18.34	21.74
12(d)	10.13	8.75	12.75	12.65	24.12	20.55	22.03
12(e)	17.12	18.72	19.67	16.17	9.55	19.53	17.44
12(f)	17.06	19.04	21.22	19.85	25.55	31.86	34.10
12(cage)	3.60	0.00	3.52	4.22	24.59	12.24	13.83
12(closo)	0.00	1.60	0.00	0.00	0.00	0.00	0.00
MAX	17.04	19.38	16.62	14.75	10.75	3.40	
RMS	11.42	13.29	10.70	10.43	7.05	1.98	

^b See Eq. 14.

TABLE VII. Relative energies (in kcal/mol) for the seven lowest $\text{Si}_{12}\text{C}_{12}$ clusters using DFT as compared to CCSD:: $\Delta_3(\text{T})$ at the MBPT(2)/cc-pVTZ reference geometry.

TABLE VIII. Relative energies (in kcal/mol) for the seven lowest $\text{Si}_{12}\text{C}_{12}$ clusters using density-fitted resolution-of-the-identity double-hybrid DFT as compared to $\text{CCSD}::\Delta_3(\text{T})$ at the MBPT(2)/cc-pVTZ reference geometry.

Si_nC_n	B2PLYP	B2GP-PLYP	DSD-BLYP	DSD-PBEP86	PWPB95	MBPT(2) ^a	CCSD:: $\Delta_3(\text{T})$ ^b
	-D3	-D3	-D3	-D3	-D3		
12(b)	17.24	19.33	21.81	20.57	18.86	28.54	19.21
12(c)	21.32	22.45	23.22	21.75	20.61	19.48	21.74
12(d)	19.47	21.48	23.10	22.32	21.92	24.12	22.03
12(e)	15.61	14.81	15.03	14.97	18.24	9.55	17.44
12(f)	28.91	31.00	31.71	31.50	34.54	25.55	34.10
12(cage)	12.93	14.96	17.33	16.22	15.25	24.59	13.83
12(closo)	0.00	0.00	0.00	0.00	0.00	0.00	0.00
MAX	5.19	3.10	3.50	2.60	1.42	10.75	
RMS	2.44	1.63	2.20	1.71	0.78	7.05	

^a Single point computed with the cc-pVQZ basis.

^b See Eq. 14.

Si_nC_n	CCSD(T) ^a	MBPT(2)::		CCSD::		CCSD::
		$\Delta_2\text{CC}$	Δ_{FNOCC}	$\Delta_2(\text{T})$	$\Delta_{\text{FNO}}(\text{T})$	$\Delta_3(\text{T})$
12(b)	17.85	19.08	19.41	18.85	19.49	19.21
12(c)	18.34	20.43	20.55	21.47	21.74	21.74
12(d)	20.55	21.69	21.84	21.79	22.07	22.03
12(e)	19.53	17.75	17.73	17.80	17.37	17.44
12(f)	31.86	32.79	33.32	33.91	34.13	34.10
12(cage)	12.24	14.01	13.83	13.42	13.90	13.83
12(closo)	0.00	0.00	0.00	0.00	0.00	0.00
MAX	3.40	1.31	1.19	0.41	0.28	
RMS	1.98	0.73	0.56	0.29	0.11	

^a Single point computed with the cc-pVTZ basis

TABLE IX. Coupled-cluster CBS relative energies (in kcal/mol) for the seven lowest $\text{Si}_{12}\text{C}_{12}$ clusters using the MBPT(2)/cc-pVTZ reference geometry. See text for details of the extrapolation methods used.